EFFECT OF LEO EXPOSURE ON AROMATIC POLYMERS CONTAINING PHENYLPHOSPHINE OXIDE GROUPS

K.A. Watson[1], S. Ghose[2†], P.T. Lillehei[2], J.G. Smith, Jr. [2], and J.W. Connell[2*]

[1]National Institute of Aerospace
100 Exploration Way
Hampton VA 23666

[2]National Aeronautics and Space Administration
Langley Research Center
Hampton VA 23681-2199

[†]NASA Postdoctoral Program Fellow

Abstract

As part of the Materials on The International Space Station Experiment (MISSE), aromatic polymers containing phenylphosphine oxide groups were exposed to low Earth orbit (LEO) for approximately 4 years. All of the aromatic polymers containing phenylphosphine oxide groups survived the exposure despite the high fluence of atomic oxygen that completely eroded other polymer films such as Kapton® and Mylar® of comparable or greater thickness. The samples consisted of a colorless polyimide film and a poly(arylene ether benzimidazole) film and thread. The samples were characterized for changes in physical properties, thermal/optical properties (i.e. solar absorptivity and thermal emissivity), surface chemistry (X-ray photoelectron spectroscopy), and surface topography (atomic force microscopy). The data from the polymer samples on MISSE were compared to samples from the same batch of material stored under ambient conditions on Earth. In addition, comparisons were made between the MISSE samples and those subjected to shorter term space flight exposures. The results of these analyses will be presented.

Keywords: Atomic oxygen resistant polymers, Self-passivating polymers, Vacuum ultraviolet radiation resistant polymers

* To whom correspondence should be addressed: john.w.connell@nasa.gov, (757) 864-4264

1. INTRODUCTION

Aromatic polymers containing phenylphosphine oxide groups have been under investigation for over a decade [1-4]. This functional group has been incorporated into a variety of aromatic polymers as a means of providing both solubility and high glass transition temperature (Tg) without sacrificing mechanical properties. It was also discovered that this group can improve the resistance of the polymer to oxygen plasma and atomic oxygen (AO) by a self passivating effect in which a phosphate enriched surface layer is formed which protects the underlying material from further reaction. A variety of experiments relating to the effects of oxygen plasma and AO exposure on these types of polymers have been performed over the years in both ground-based simulations and short term space flight exposure experiments [5-9]. Until now, there has been no data available regarding the long term (> 1 year) performance of these types of polymers in low Earth orbit (LEO).

The push to develop AO resistant polymers dates back to pre-space station days and since that time a variety of approaches have been investigated. Some of the early work involved polyphosphazenes [10,11]. In addition, a large variety of silicon (Si) containing polymers were investigated in which the Si was typically incorporated in the form of an organic species such as a siloxane unit [12-21]. In both cases, the formation of an oxide rich surface layer by the reaction of phosphorus (P) or Si with atomic oxygen was observed. This oxide surface layer reduced the subsequent reaction efficiency with AO and protected the underlying polymeric material. Other approaches involved highly fluorinated polymers [13, 22-23] or coatings such as aluminum oxide [24], silicon oxide [24], chromium oxide [23], and indium tin oxide [25]. Certain disadvantages exist with coatings such as the formation of defects during application, difficulty in coating large or complex shapes, cracking and spalling due to thermal cycling caused by differences in thermal expansion between coating and substrate, micrometeoroid and debris impacts, and poor adhesion to the substrate.

More recent work has focused on the incorporation of polyhedral oligomeric silsesquioxanes (POSS) molecules into polymers as a means of achieving AO resistance. POSS molecules are caged silicates typically represented by the formula Si_8O_{12} wherein organic functional groups can be attached to one or more of the Si atoms. The functional groups are designed so that they can react with specific monomers such that POSS molecules become incorporated into the polymer backbone at a molecular level. A polyimide containing 31 weight percent POSS exhibited excellent performance in ground-based simulated AO exposure tests [26-28]. As with other Si containing polymers, the AO resistance is attributed to the reaction of AO with the Si in the material leading to the formation of a silicon oxide enriched surface layer which subsequently decreases the reaction rate with AO thereby protecting the underlying polymer.

The Materials on The International Space Station Experiment (MISSE) program is a combined effort primarily between NASA, The Air Force Research Laboratory, and Boeing Phantom Works. The MISSE 1 and 2 flight experiments consisted of two passive experiment carriers [PEC, (also referred to as suitcases)] of material specimens

that were attached to the International Space Station and passively exposed to the LEO space environment [i.e., AO, ultraviolet (UV) radiation, particulate radiation, thermal cycling, and the induced environment of the space station]. The materials were deployed in August 2001 and were intended to experience a one year exposure. Due to the Space Shuttle Columbia accident in February 2003 and subsequent delays in returning to flight, the PECs were not retrieved until August 2005. Consequently, many polymer samples were completely eroded by AO including Kapton® HN film [127 microns (μm) or 5 mils thick]. One suitcase was intended to experience exposure in the flight (RAM) direction and the other in the WAKE direction. However, due to the orbital configuration of the International Space Station, the WAKE exposed samples experienced more AO fluence than expected. A report is available detailing the exposure conditions experienced by the hardware and material specimens during this flight experiment [29]. The results of this space flight exposure, particularly of AO exposure, on some aromatic polymers containing phenylphosphine oxide groups will be presented.

2. EXPERIMENTAL

2.1 Materials The polymers consisted of a colorless polyimide film and a poly(arylene ether benzimidazole) film and thread. The polyimide film was prepared in the laboratories of the Advanced Materials and Processing Branch, NASA Langley Research Center following a procedure previously reported [30]. The poly(arylene ether benzimidazole) film (TOR-LM) was metallized with a 100 nm thick coating of vapor deposited aluminum (VDA). The film (38 μm or 1.5 mil thick) was mounted such that the polymer surface faced the orbital velocity direction (RAM). Both the TOR-LM film [9] and thread (TOR) [6] were obtained from Triton Systems, Inc. in 2000. Additional samples fabricated from the TOR family of polymers, provided by other principal investigators, were also flown on this flight experiment. These samples consisted of woven fabrics and tethers.

2.2 Flight Exposure Conditions The film sample dimensions were 10.2 cm x 10.2 cm (4 in x 4 in) and 25 to 40 μm thick. They were mounted on an aluminum plate and held in place with strips of metal on two sides that were bolted down. The conditions experienced during the nearly four year exposure for this set of samples (RAM facing side) were as follows: AO fluence from 6.5 to 9.1 x 10^{21} atoms/cm^2; equivalent solar hours 5870 to 6134 depending on exact sample location; thermal cycling, minimum temperature ~ -55 ºC, maximum temperature ~ 66 ºC, average temperature -13ºC. Most thermal cycles were from -30 ºC to +40 ºC. The normal orbital period was around 90 minutes. PECs inspected by black light after exposure appeared to be very clean and contamination was deemed minimal. For more detailed information concerning the exposure conditions, please see reference 29.

2.3 Characterization Prior to integration, samples were tested for total mass loss (TML) and collected volatile condensable material (CVCM) by heating to 125ºC under vacuum

of (10^{-6} Torr) for 24 h. The temperature of the collection plate was 25ºC. The samples were equilibrated at 50% relative humidity prior to weighing. The samples were also tested for flammablility using the UL-94 test method. Fourier transform infrared (FTIR) spectroscopy was performed on a Nicolet Magna-IR 560 ESP spectrometer on thin films or as KBr pellets. The percent light transmission through the thin films was measured at 500 nm using a Perkin-Elmer Lambda 900 UV/VIS/NIR spectrometer. Solar absorptivities (α) of thin films were measured on an AZTek Model LPSR-300 spectroreflectometer with measurements taken between 250 to 2800 nm using a vapor deposited aluminum on Kapton® film (1^{st} surface mirror) as a reflective reference per ASTM E903-82. An AZTek Temp 2000A infrared reflectometer was used to measure the thermal emissivity (ε) of thin films. X-ray photoelectron spectroscopy (XPS) was performed using a VG XPS system having an analysis chamber equipped with an 80 L/s ion pump yielding a base pressure of $< 1 \times 10^{-9}$ Torr and an electron flood gun for charge compensation. The system was calibrated by aligning measured peak energies of an elemental gold sample with known values. The preparation chamber was pumped using a 100 L/s turbo pump. For analysis, 1253 eV X-rays from a magnesium anode were used and photo-electron energies were resolved using a hemispherical energy analyzer having a resolution of 0.2 eV at a pass energy of 20 eV. A set of ten survey scans with a step size of 1 eV, a pass energy of 50 eV, and a dwell time of 100 ms was performed. This was followed by 20 scans for C 1s, N 1s, O 1s and P $2p_{3/2}$ peaks. The step size for the four high-resolution scans was 0.1 eV with a pass energy of 50 eV and a dwell time of 200 ms. Because the samples were insulating materials, charge compensation had to be performed using a current of 0.01 mA at 2 eV from the electron flood gun. Atomic force microscopy (AFM) was performed on the film and thread samples using a Digital Instruments MultiMode Scanning Probe Microscope (Veeco Metrology, Inc.). The samples were imaged in TappingMode and analyzed for surface roughness. Both the average roughness (R_a) and the root mean square roughness (R_q) were recorded at several locations per sample [31].

3. RESULTS AND DISCUSSION

3.1 Materials The chemical structures of the aromatic polymers containing phenylphosphine oxide groups are presented in Figure 1.

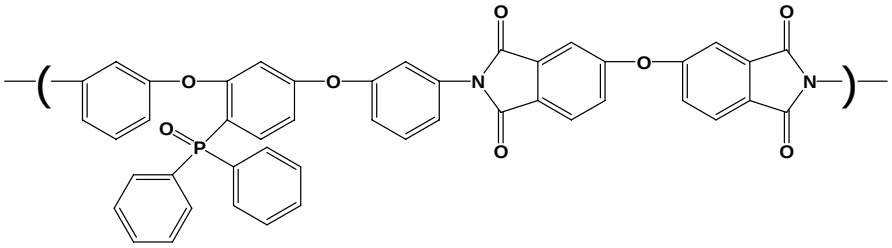

Colorless Polyimide

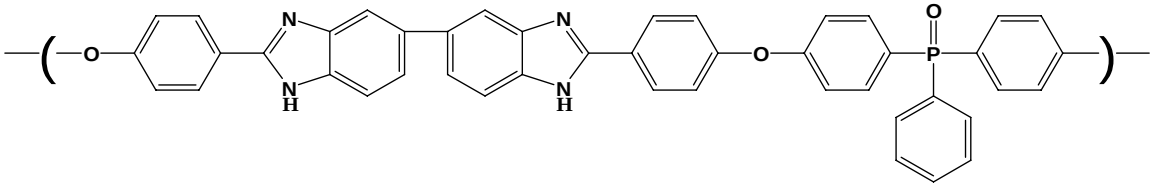

TOR

TOR-LM is a 1:1 random copolymer of TOR (chemical structure above) with 4,4'-biphenol.

Figure 1. Chemical structure of polymer samples.

The polymer samples were mounted in the exposure tray as shown in Figure 2.

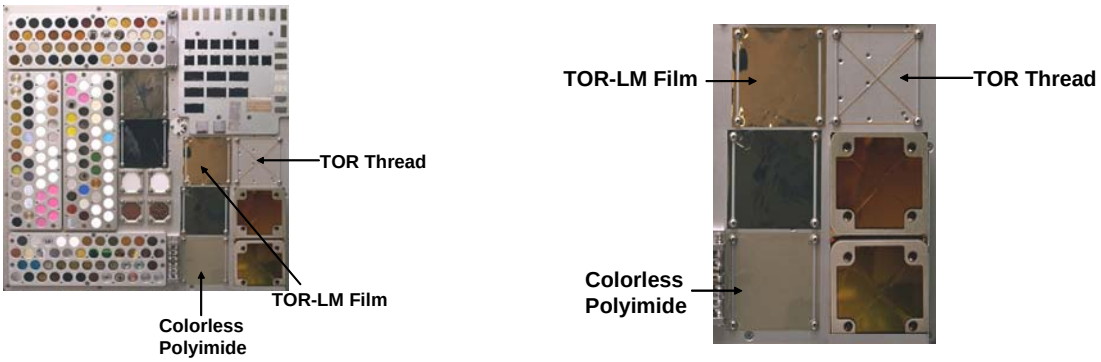

a b

Figure 2. (a) Samples mounted on exposure tray; (b) Enlarged image of samples

As shown in Figure 2, metal bars on two sides of each film held them against the backing plate. Control films and threads were cut from the same batch of material as that used in

the flight experiment. The control samples were maintained in zip-lock bags under ambient conditions until the return of the flight specimens.

3.2 Flight Exposure Conditions It is important to recognize that the flight samples were exposed to LEO where there is no molecular oxygen or water vapor. When returned to Earth for analysis, the samples were exposed to the ambient atmosphere which contains both molecular oxygen and water vapor. Thus, the potential exists for the surface chemistry to have been affected by this exposure.

The exposure experiment was originally intended to last for one year, but ended up lasting nearly four. Consequently many samples did not survive the high AO fluence. For example, relatively thick (127 μm) Kapton® HN samples were completely eroded. Other polymer films such as Mylar®, metallized polyimides, and polybenzoxazole were also completely eroded. The flight samples were exposed to an AO fluence of 6.5 to 9.1 x 10^{21} atoms/cm^2 with simultaneous exposure to thermal cycling and UV and particulate radiation.

Aromatic polymers containing phenylphosphine oxide groups have previously been exposed to both ground-based simulated AO as well as AO in short term space flight exposure experiments. From these experiments a few general conclusions were derived. Upon exposure to AO aromatic polymers containing phenylphosphine oxide groups generally exhibit a two stage erosion process. In the first stage material is lost via the reaction of AO with the polymer surface to form small organic molecules that are subsequently lost via volatilization, which is typical of most organic polymers. Simultaneously the AO exposed surface becomes enriched with a phosphate layer, eventually forming a polyphosphate surface layer. In the second stage AO erosion is significantly lessened due to the reduced reactivity between the polyphosphate layer and AO. Evidence for this comes from the erosion rate, XPS, ^{31}P nuclear magnetic resonance (NMR) spectroscopy, and X-ray adsorption near edge spectroscopy (XANES) analyses [2-8, 32].

In ground-based AO simulation facilities there are differences in the flux and energy level of AO. In some of these facilities, reactive species other than AO are present and can increase the degradation of the material. In addition, the samples are not simultaneously exposed to UV and particulate radiation and thermal cycling. Thus it seems more valid to compare the results of this MISSE experiment with other space flight exposure experiments. In prior space flight exposure experiments involving aromatic polymers containing phenylphosphine oxide groups the samples were exposed to AO fluences of 7 x 10^{19} atoms/cm^2 [5, 7] and 1 x 10^{19} atoms/cm^2 [8]. Based on these results, it was determined that aromatic polymers containing phenylphosphine oxide groups had a reaction efficiency of about 15 times less than that of Kapton® HN.

3.3 Visual Inspection of Flight Specimens Samples were returned to NASA Langley Research Center in October 2005 and placed in a clean room for observation and subsequent deintegration. Pictures of the returned specimens still mounted in the PEC

are presented in Figure 3. As can be seen from the image, the film samples were intact. The TOR-LM film sample had two small cracks adjacent to the metal bars holding the sample against the plate. Whether these cracks were due to stress build-up as a result of the thermal expansion mismatch between the metal bars and the polymer, or from material degradation is not known. Both the TOR-LM and colorless polyimide film samples appeared diffuse or "frosted" as a result of AO erosion and were no longer transparent. There was no visible erosion or obvious deterioration of the thread sample. The samples were subsequently removed from the tray for additional characterization. Surprisingly, the materials were not brittle or fragile and did not suffer further deterioration upon handling and manipulation. Both films exhibited sufficient toughness such that they could be creased without visible damage, cracking, or fracture. In comparing these visual results with those from previous flight experiments [5,7,8], the previous samples were not visibly frosted and remained transparent, however the AO fluence was only in the range of 1-7 x 10^{19} atoms/cm^2.

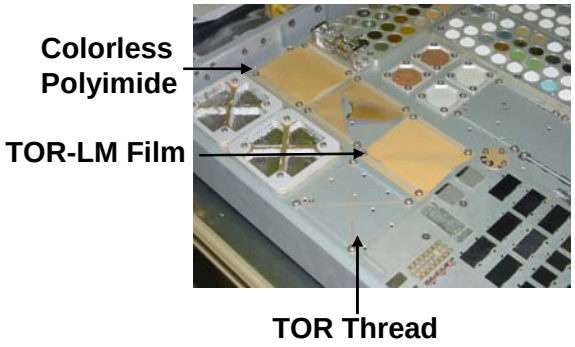

Figure 3. Samples after return

3.4. Characterization Outgassing and flammability tests were performed on the unexposed film and thread samples (Table 1). All samples exhibited very low outgassing and, as expected due to their aromatic structure, were nonflammable.

Table 1. Outgassing/Flammability Results

Sample	TML, Weight%	CVCM, Weight%	UL-94
TOR Thread	0.25	0	0
Colorless Polyimide	0.16	0.02	0
TOR-LM	0.25	0	0

FTIR was performed on samples of the colorless polyimide and TOR-LM films. In the polyimide film, the carbonyl peaks readily visible in the spectra corresponding to the control sample are significantly dampened in the spectra of the exposed film. This was the general trend for the bulk of the other significant FTIR spectral features as well as for the control and exposed TOR-LM films. Optical transparency at 500 nm was measured on the colorless polyimide films. The control sample exhibited a transparency of ~84% whereas the flight specimen was <1%. The sample was visibly frosted or opaque thus the

low transparency was due to the scattering of light by the eroded film surface. Solar absorptivity (α) and thermal emissivity (ε) data was collected on samples of the colorless polyimide and TOR-LM films (Table 2). Solar absorptivity increased significantly due to the AO exposure. The increase in α for the colorless polyimide film was the same for the RAM facing side as well as the backside of the film. The samples were also darker in color, had a diffuse appearance and were no longer transparent. The polymer surface of the TOR-LM film exhibited a larger increase in ε than the colorless polyimide film. The exposed backside of the TOR-LM film, which had a VDA surface, did not exhibit any changes in α or ε.

Table 2. Solar Absorptivity/Thermal Emissivity

Sample	α	ε	α/ε
Colorless Polyimide control	0.07	0.67	0.11
Colorless Polyimide exposed backside	0.23	0.71	0.32
Colorless Polyimide RAM facing side	0.23	0.76	0.30
TOR-LM control (polymer surface)	0.31	0.71	0.44
TOR-LM control (VDA surface)	0.08	0.04	2.0
TOR-LM exposed backside (VDA surface)	0.08	0.04	2.0
TOR-LM RAM facing side (polymer surface)	0.50	0.85	0.59

As a means to investigate changes in surface chemistry, XPS was performed on the polymer samples including the thread. The typical analysis depth is 2 to 5 nm, depending on the material, and a particular element (except hydrogen) can be measured down to 0.1% atomic fraction. The experiments were performed on both sides of each film. By summing the area under the photoelectron peaks corresponding to different elements, the concentrations of those elements were determined(Tables 3-5).

Table 3. XPS Analysis Results for TOR Thread

Photoelectron	Control, Atomic Concentration %	Exposed, Atomic Concentration %
O 1s	19.3	26.7
N 1s	11.9	20.4
C 1s	67.8	51.3
P 2p	1.0	1.5

Table 4. XPS Analysis Results for the Colorless Polyimide

Photoelectron	Control, Atomic Concentration %	RAM Exposed, Atomic Concentration %	Backside Exposed, Atomic Concentration %
O 1s	16.3	46.5	36.4
N 1s	3.2	3.4	4.1
C 1s	78.9	38.1	51.3
P 2p	1.6	12.0	8.2

Table 5. XPS Analysis Results for TOR-LM

Photoelectron	Control, Atomic Concentration %	Exposed, Atomic Concentration %
O 1s	11.5	44.1
N 1s	2.1	4.7
C 1s	83.6	41.4
P 2p	2.7	10.0

To summarize the results form the XPS analyses, for each sample there is a noticeable increase in the oxygen and phosphorus concentration after exposure. The high resolution O 1s signal from the samples could be fit with two peaks corresponding to two different bonding situations. The O 1s sub-peak at 530 eV is reduced while the sub-peak at 534 eV increases indicating that the oxygen has become more strongly bound (i.e. it is more inorganic). After exposure the amount of phosphorus at the surface has increased. This is most likely in the form of an oxide (phosphate) since the binding energy of the P $2p_{3/2}$ peak shifts from 132 eV to 135 eV. The amount of carbon is reduced presumably due to loss of material via reaction with AO and subsequent volatilization. There is also an increase in the nitrogen oxidation state and concentration, particularly for the thread sample. This indicates that nitrogen was also retained in the surface of these materials, probably in the form of a nitride. In the case of the colorless polyimide, the changes in surface chemistry follow the same trend as those on the RAM facing side indicating that AO had access to the backside of the film. Changes in surface chemistry are due to reaction of polymeric material with AO and are consistent with those observed on other ground-based and short term flight exposure experiments.

AFM analyses were performed on the samples to investigate changes in surface topography. All samples showed an increase in surface roughness upon exposure both on the exposed backside and the RAM facing side. The results are presented in Table 6.

Table 6. AFM analysis of surface roughness

Sample	Average R_a (nm)	Standard Deviation of R_a (nm)	Average R_q (nm)	Standard Deviation of R_q (nm)
Colorless Polyimide control	0.466	0.024	0.733	0.075
Colorless Polyimide exposed backside	8.443	7.486	12.01	9.842
Colorless Polyimide RAM facing side	419.1	371.7	517.1	452.1
Colorless Polyimide RAM facing side (under metal bar)	80.21	80.66	99.17	95.40
TOR-LM exposed backside	1.757	0.704	2.364	1.435
TOR-LM exposed RAM facing side	427.4	206.0	525.2	245.0
TOR-LM exposed RAM facing side (under metal bar)	326.8	172.3	408.1	209.5

Samples were also examined on the exposed side in the area that was covered (protected) by the metal mounting bars. Both film samples showed a significant increase in surface roughness on the RAM facing side when compared to the control sample. The exposed

backside of the colorless polyimide film showed an increase in roughness compared to both the control and the exposed backside of TOR-LM. This is consistent with the XPS results showing that the exposed backside of the colorless polyimide film did experience exposure to AO. The exposed backside of the TOR-LM did not exhibit as much erosion, but still had an increase in roughness compared to the control. The difference in observed erosion for these two samples was likely influenced by the backside of the TOR-LM film having a VDA surface. It was also observed that the exposed backside of the TOR-LM film was similar to polymer samples that have been track etched by exposure to an alpha source [33]. As the high energy alpha particles penetrated the sample they left track marks that were clearly visible on the back side of the sample (Figure 4).

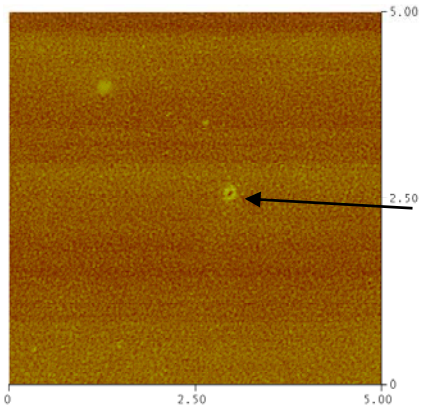

Figure 4. AFM image of TOR-LM exposed backside showing increased surface roughness and track marks (denoted by arrow). X and Y axis units are in μm.

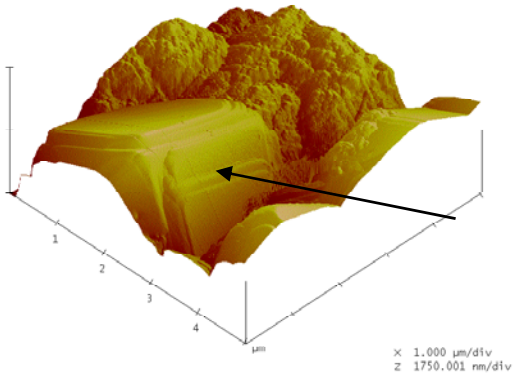

Figure 5. AFM image of the TOR-LM exposed RAM facing surface showing platelet formation (denoted by arrow). X and Y axis units are in μm.

Tthe exposed RAM facing surface of TOR-LM film showed what appeared to be platelet formations that served as etch stops in the material (Figure 5). Even though the RAM facing surface was significantly roughened, the platelets seemed to slow the etching where they formed. It is important to note that the average surface roughness and the

relative standard deviation of the roughness both increased. This indicates that the sample did not roughen in a homogeneous fashion, consistent with the theory that the sample forms platelets that are comprised of a phosphate material that act as an etch stop.

The exposed thread samples showed a decrease in the overall diameter, separation of the weave, and an increase in surface roughness, but the data cannot be quantified due to the uneven surface features of both the unexposed and exposed threads. Qualitatively, the thread sample was not noticeably degraded and could not be readily broken by hand.

4. SUMMARY

As part of the MISSE flight experiment aromatic polymers containing phenylphosphine oxide groups were exposed to LEO for approximately four years. The polymers survived intact despite high AO fluence (6.5 to 9.1 x 10^{21} atoms/cm^2) whereas other polymers such as Kapton®, Mylar®, and metallized polyimides were completely eroded. The polymer films appeared visibly frosted due to AO erosion, whereas there were no visible changes in the thread. AO erosion significantly affected optical transparency as well as solar absorptivity and thermal emissivity of the film samples. The changes in surface chemistry as determined by XPS were consistent with the formation of a phosphate (i.e., phosphorus oxide) surface layer. Changes in surface topography consistent with AO erosion were evident from AFM analysis. The effects of this exposure on aromatic polymers containing phenylphosphine oxide groups are consistent with those previously reported from shorter term space flight exposure experiments. Due to the changes in properties exhibited by the films, these materials are perhaps more suitable for applications on spacecraft in LEO in the form of stitching thread, woven fabric, softgoods, or tethers.

5. ACKNOWLEDGEMENT

The authors would like to gratefully acknowledge Drs. Brian C. Holloway and Randy Collette from the Applied Science Department at the College of William and Mary for performing the XPS analyses.

6. REFERENCES

1. C.D. Smith, H. Grubbs, H.F. Webster, A. Gungor, J.P. Wightman and J.E. McGrath, High Performance Polymers, 3(4), 211 (1991).
2. J.G. Smith, Jr., J.W. Connell and P.M. Hergenrother, Polymer, 35(13), 2834 (1994).
3. J.W. Connell, J.G. Smith, Jr. and P.M. Hergenrother, Polymer, 36(1), 5 (1995).
4. J.W. Connell, J.G. Smith, Jr. and J.L. Hedrick, Polymer, 36(1), 13 (1995).

5. J.W. Connell, J.G. Smith, Jr., C.G. Kalil and E.J. Siochi, Polymers for Advanced Technologies, 9(1), 11 (1998).
6. P. Schuler, R. Haghighat and H. Mojazza, High Performance Polymers, 11(1), 113 (1999).
7. J.M. Zwiener, R.R. Kamenetzky, J.A. Vaughn, M.M. Finckenor and P. Peters, MIR-ISSA Risk Mitigation Flight Experiment RME One-Year Final Report, http://setas-www.larc.nasa.gov/meep/1-year/posa_I/posa1_1_year.html
8. J.W. Connell, High Performance Polymers, 12(1), 43 (2000).
9. P. Schuler, H. Mojazza and R. Haghighat, High Performance Polymers, 12(1), 113 (2000).
10. L.L. Fewell, J. App. Polym. Sci., 41, 391 (1990).
11. L.L. Fewell and L. Finney, Polymer, 32, 393 (1991).
12. W.S. Slemp, B. Santos-Mason, G.F. Sykes, Jr. and W.G. Witle, Jr., AO Effect Measurements for Shuttle Missions STS-8 and 41-G, 1(5), 1 (1985).
13. L.J. Leger, J.T. Visentine and B. Santos-Mason, SAMPE Q, 18(2), 48 (1987).
14. J.T. Visentine, L.J. Leger, J.F. Kuminecz and K.I. Spiker, AIAA 23rd Aerospace Conf Proc., AIAA-85-7021 (1985).
15. C.A. Arnold, J.D. Summers, Y.P. Chen, R.H. Bott, D.H. Chen and J.E. McGrath, Polymer, 30, 986 (1989).
16. C.A. Arnold, J.D. Summers, Y.P. Chen, T.H. Yoon, B.E. McGrath, D.H. Chen and J.E. McGrath, in 'Polyimides: Materials, Chemistry and Characterization" (Ed. C. Feger), Elsevier Science Publishers, Amsterdam, 1989 pp. 69-89.
17. C.A. Arnold, D.H. Chen, Y.P. Chen, R.O. Waldbauer, Jr., M.E. Rogers and J.E. McGrath, High Performance Polymers, 2(2), 83 (1990).
18. J.W. Connell, D.C. Working, T.L. St. Clair and P.M. Hergenrother, in 'Polyimides: Materials, Chemistry and Characterization" (Ed. C. Feger), Technomic, Lancaster, PA, 1993 pp. 152-164.
19. J.W. Connell, J.G. Smith, Jr. and P.M. Hergenrother, J. Fire Sci., 11(2), 137 (1993).
20. P.R. Young and W.S. Slemp, in "NASA CP 3162 Part 1", 1991 pp. 376-378.
21. J. Kulig, G. Jefferis and M. Litt, Polym. Mater. Sci. Eng., 61, 219 (1989).
22. A.E. Stiegman, D.E. Brinza, M.S. Anderson, T.K. Minton, G.E. Laue and R.H. Liang, Jet Propulsion Laboratory Publication 91-10, May (1991).
23. L.J. Leger, K.I. Spikes, J.F. Kuminecz, T.J. Ballentine and J.T. Visentine, "STS Flight 5, LEO Effects Experiment", AIAA-83-2631-CP (1983).
24. B.A. Banks, M.J. Mistich, S.K. Rutledge and H.K. Nahra, Proc. 18th IEEE Photovoltaic Specialists Conf., (1985).
25. K.A. Smith, "Evaluation of Oxygen Interactions with Materials, STS-8 AO Effects", AIAA-85-7021 (1985).
26. J.W. Gilman, D.S. Schlitzer and J.D. Lichtenhan, J. App. Polym. Sci., 60, 591 (1996).
27. A.L. Brunsvold, T.K. Minton, I. Gouzman, E. Grossman and R. Gonzalez, High Performance Polymers, 16(2), 303 (2004).
28. M.E. Wright, B.J. Petteys, A.J. Guenthner, S. Fallis, G.R. Yandek, S.J. Tomczak, T.K. Minton and A.L. Brunsvold, Macromoloecules, 39, 4710 (2006).
29. G. Pippin, Final Report Air Force Contract 02-S470-011-C1, July 2006.

30. K.A. Watson, F.L. Palmeri and J.W. Connell, Macromolecules, 35, 4968-4974 (2002).
31. ISO 4287-1997, ISO 4288-1996
32. J.W. Connell, J.G. Smith, Jr. and P.M. Hergenrother, in 'High Temperature Properties and Applications of Polymeric Materials", ACS Symposium Series 603 (M.R. Tant, J.W. Connell and H.L.N. McManus, Editors), American Chemical Society, Washington, DC, 1995 pp. 186-199.
33. Kamlendra Awasthi, V. Kulshrestha, N.K. Acharya, M. Singh and Y.K. Vijay, European Polymer Journal, 42, 883–887 (2006).